Strain and piezoelectric fields in arbitrarily oriented semiconductor heterostructures. II. Quantum wires

Liberato De Caro and Leander Tapfer
Centro Nazionale Ricerca e Sviluppo Materiali (CNRSM), Strada Statale 7 Appia, kilometer 712, I-72100 Brindisi, Italy
(Received 5 July 1994; revised manuscript received 25 October 1994)

In this paper, we investigate the strain and piezoelectric fields of semiconductor quantum-wire heterostructures. The quantum-wire structures considered here are those which are fabricated from superlattices grown on a thick substrate crystal and are laterally confined by vacuum or air. The strain-tensor components are calculated by minimization of the strain-energy density and by imposing the commensurability constraint at the wire/substrate interface only along the wire direction. In fact, due to the finite lateral dimension of the structure, a relaxation of the crystal lattice perpendicular to the wire occurs until the minimum of the strain energy is reached. A detailed study of the symmetry of the distorted crystallographic unit cell as a function of the substrate orientation and the wire direction is presented. We find that due to the anisotropic elastic lattice relaxation of the quantum wires a lower-symmetry lattice deformation than a tetragonal one can occur also for the [001]-substrate orientation. We show that, for zinc-blende heterostructure quantum wires, these strain fields can generate high piezoelectric fields that can be different from zero even for the high-symmetry [001]-interface orientation. Due to the presence of these high piezoelectric fields in quantum-wire structures, a one-dimensional electron gas can be produced.

I. INTRODUCTION

It is well known that strain fields, generated by the lattice mismatch between different material systems of semiconductor heterostructures (HS's), affect both their microscopic[1,2] and macroscopic physical properties.[3] In the case of layered structures, which are grown pseudomorphically on thick substrate crystals, the elastic lattice deformation is characterized by the evidence that the in-plane lattice mismatch between film and substrate is zero, i.e., the lattice constant of the HS's is accommodated to the lattice parameter of the substrate in all in-plane directions[4] (see paper I of this work).

Elastic-relaxation phenomena, which modify strain fields, are observed in semiconductor structures with reduced spatial dimensions.[5–7] In particular, lattice relaxation may play a very important role for low-dimensional systems, such as quantum-wire superlattices (QWSL's), which are of great current interest due to their unique physical properties and potential optoelectronic-device applications. Recently, we have shown that the experimentally observed strain fields[5,6] can be accounted for by considering the quantum-wire superlattices as an alloy and by using the elasticity theory and the appropriate boundary conditions.[8]

In this paper, the strain status of one-dimensional (1D) HS's with cubic symmetry, fabricated on arbitrarily oriented thick substrate crystals with a different lattice constant, has been determined by minimizing the strain-energy density via the commensurability constraint (Sec. II). In Sec. III, the lattice deformations have been calculated and analyzed as a function of the substrate orientation and the wire direction. Here, the QWSL's are not considered as an alloy,[8] but the strain fields of the individual layers of the QWSL period are calculated. Furthermore, important differences with respect to the superlattice (SL) case (reported in paper I of this work) are elucidated and discussed. Finally, in Sec. IV the piezoelectric fields generated by the strain fields are calculated and discussed. In particular, relaxation phenomena can lead to strain-induced electric fields also for the [001] substrate orientation, in contrast with the 2D HS's (SL case).

II. LATTICE COMMENSURABILITY CONSTRAINT

The quantum-wire heterostructures considered here are fabricated from SL's that are grown on thick substrate crystals [Fig. 1(a)]. After a lithographic patterning followed by a dry or wet etching, thin parallel stripes are obtained. The sidewalls of the quantum wires are exposed to air or vacuum [Fig. 1(b)] and no lateral stress is

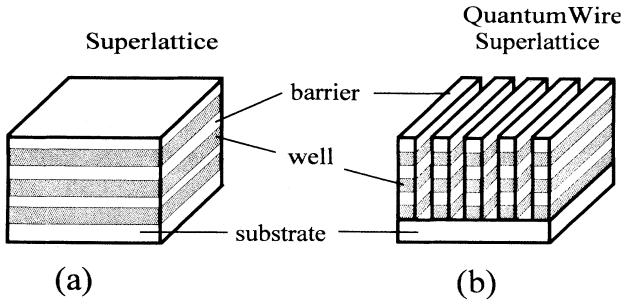

FIG. 1. Schematic diagram of a superlattice (a) and a quantum-wire heterostructure (b). The quantum-wire array is fabricated from a superlattice, which is grown epitaxially on a thick substrate crystal, by lithographic patterning followed by an etching process.

induced as may occur in regrown or embedded structures.

Now, let us consider two semiconductor materials, both of cubic-crystal symmetry, which constitute a SL. By reducing one lateral dimension in order to obtain a quantum-wire structure, a relaxation of the quantum-wire lattice occurs that modifies the strain fields.[5–8] Therefore, even if the SL has been grown coherently on an arbitrarily oriented thick substrate crystal, after the quantum-wire fabrication we cannot assume anymore that the in-plane lattice constant of the wire must be the same as for the substrate for any arbitrary direction in the interface plane. In fact, even after the lattice deformation, if no plastic deformation occurs, i.e., no generation of misfit dislocations at the wire-substrate interface, the lattice translation vectors of each strained material must have a common projection onto the growth plane (lattice commensurability constraint) only along the wire direction.[8] Defining the distorted lattice translation vectors as introduced in paper I of this work, and by using (i) the commensurability constraint between layers a and b of one SL period of the QWSL for any direction in the interface plane, and (ii) the commensurability condition with the substrate lattice only along the wire direction, we obtain the following relations:

$$\begin{aligned} & d_a \bar{\varepsilon}^{\,a}_{12} = d_b \bar{\varepsilon}^{\,b}_{12} , \\ & d_a(\bar{\varepsilon}^{\,a}_{11}+1) = d_b(\bar{\varepsilon}^{\,b}_{11}+1) , \\ & d_a(\bar{\varepsilon}^{\,a}_{22}+1) = d_b(\bar{\varepsilon}^{\,b}_{22}+1) = d_s . \end{aligned} \tag{1}$$

Here, the $\bar{\varepsilon}^{\,a}_{ij}$ are the strain-tensor components with respect to the interface reference system x'_1, x'_2, and x'_3 as shown in Fig. 2. The axis x'_2 is directed along the wire, while the axis x'_3 is normal to the interface between the quantum wire and substrate. Thus, we can impose only one further condition with respect to the free-standing SL case (see paper I). It must be noted that, in real cases, Eqs. (1) should not be valid in the region near the interface, where the coherence condition is fulfilled for all the in-plane directions (see Fig. 2). In other words, the strain field cannot be considered uniform everywhere in layers a and b of the HS. However, experimental high-resolution x-ray diffraction evidenced that in real 1D HS's the lattice deformation can be successfully described by only the coherence boundary condition along the wire direction, depending on the amount of the lattice mismatch and of the height/width ratio of the wire structure.[8,9] In this way, the strain field can be considered uniform almost everywhere except for a few monolayers near the interface, where the strain changes gradually in order to allow the matching of the lattice of the individual layers a and b of the strained HS with the lattice of the thick substrate for all the in-plane directions. A more rigorous strain model, which describes the elastic lattice relaxation at the quantum-wire substrate interface as a function of the distance from the interface and the width of the wires, will be reported elsewhere.[9]

III. STRAIN-FIELD CALCULATION

For the calculation of the strain fields in QWSL's we assume, in accordance with the experimental evidences,[5,6] that the lattice of layers a and b of the quantum wires are coherent with respect to the substrate lattice only along the wire direction. Along the interface direction perpendicular to the wire no coherence condition with the substrate lattice (commensurability constraint) is imposed. In order to obtain all the tensor components of the strain fields in a quantum-wire structure, the strain energy density U expressed as a function of $\bar{\varepsilon}^{\,a}_{ij}$ is minimized by using the constraints given by Eqs. (1).[10]

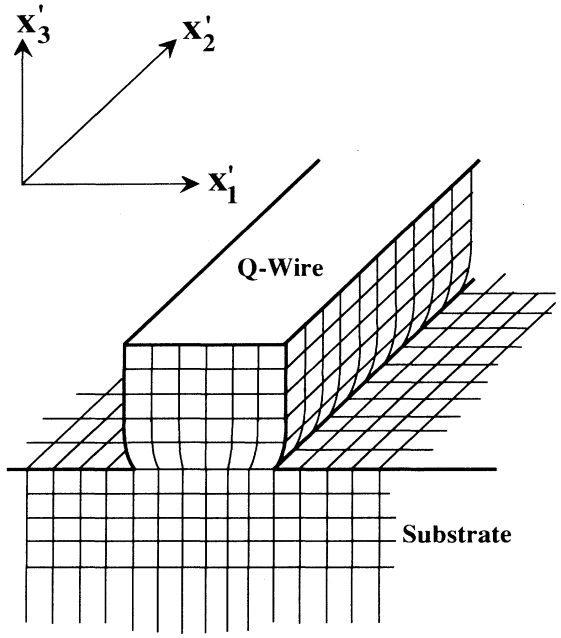

FIG. 2. Schematic diagram of the elastic lattice deformation in a strained quantum wire near the wire/substrate interface. The elastic lattice relaxation occurs perpendicular to the wire direction (x'_1), while the wire lattice is perfectly coherent with the substrate along the wire direction (x'_2).

The strain components are given in the matrix notation[11] in order to have more compact final formulas. The complete analytical expressions of the strain-tensor components are reported in the Appendix. Here, we will discuss in detail the most interesting properties of the lattice deformations. The strain field of the quantum wires caused by the lattice mismatch [see Eqs. (A1) and (A2) in the Appendix] depends on the substrate surface orientation as well as on the wire direction. It is important to note that, in the case of two-dimensional HS's (superlattices), as reported in paper I of this work,[10] we have obtained a tetragonal lattice deformation for all high-symmetry substrate orientations, i.e., [001], [110], and [111], since all the off-diagonal components of the strain tensor are equal to zero. Moreover, for low-symmetry substrate orientations the lowest-symmetry lattice deformation is monoclinic, due to the isotropy of the boundary conditions in the interface plane.

On the contrary, for lateral confined HS's (QWSL's) the situation is much more complicated, even for high-symmetry substrate orientations. In the following two subsections, we will analyze two different cases: the first

one concerns a 1D HS grown on the [001]-oriented substrate, with an arbitrary $[\bar{k}10]$ or $[\bar{1}k0]$ wire direction; the second one considers a 1D HS grown on an arbitrary $[kk1]$- or $[11k]$-oriented substrate, where the wire direction is fixed along the $[\bar{1}10]$ direction.

A. $[\bar{k}10]$- and $[\bar{1}k0]$-oriented quantum wires fabricated on [001]-oriented substrates

If the substrate surface is normal to the [001] direction, we can choose the three coordinate axes $\{x_i'\}$ as follows: $x_1' \| [jk0]$, $x_2' \| [\bar{k}j0]$ (wire direction), and $x_3' = [001]$, where j and k are integers. In particular, in Fig. 3 the lattice deformations for two families of quantum-wire orientations, namely, $[\bar{k}10]$ with k integer if $0 \le T_{22} \le 1/\sqrt{2}$ and $[\bar{1}k0]$ with k integer if $1/\sqrt{2} \le T_{22} \le 1$, are shown. The solid lines are referred to a single laterally confined $In_{0.2}Ga_{0.8}As$ layer, coherently fabricated on a thick GaAs substrate. The parameters for the ternary compound epitaxial layer are obtained from a linear interpolation of the parameters of the constituent binary compounds as reported in Ref. 12. The dashed lines are referred to the $In_{0.2}Ga_{0.8}As$ wells of a laterally confined $GaAs/In_{0.2}Ga_{0.8}As$ QWSL, coherently fabricated on a thick GaAs substrate. The curves labeled by 1 show the perpendicular component of the lattice deformation, i.e., $\varepsilon_{sb} - \bar{\varepsilon}_{33}$, while the curves labeled by 2 show the in-plane lattice deformation orthogonal to the wire direction, i.e., $\varepsilon_{sb} - \bar{\varepsilon}_{11}$. In the QWSL case, the thicknesses of the two layers of the SL period have been chosen to be equal, and as the average strain depends on the thickness ratio, it is not necessary to specify their actual values. However, the individual $In_{0.2}Ga_{0.8}As$ layer thickness and the total SL thickness should be smaller than the critical thickness.

Clearly, the presence of the GaAs barriers reduces the amount of the lateral relaxation of the wire lattice. In fact, the in-plane constant of the well is closer to the substrate value, due to the presence of the GaAs barriers. In turn, this causes the absolute value of the perpendicular lattice deformation of the HS wells (dashed curve 1) to be greater than the correspondent value for the single-layer case (solid curve 1). Figure 4 shows the only nontrivial shear strain components for the $In_{0.2}Ga_{0.8}As$ layer. The solid line refers to the single-layer case and the dashed line to the SL case. From Figs. 3 and 4 we can see that for the single-layer case, the lattice deformation is tetragonal[8] for the highest-symmetry wire direction [010], since all the shear strain components are equal to zero and $\bar{\varepsilon}_{33} = \bar{\varepsilon}_{11}$. In contrast, for the multilayer case, due to the presence of the barrier layers, the highest-symmetry lattice deformation for these families of wire directions is orthorhombic. Moreover, except for the [010] and the $[\bar{1}10]$ wire directions, all the other possible geometrical

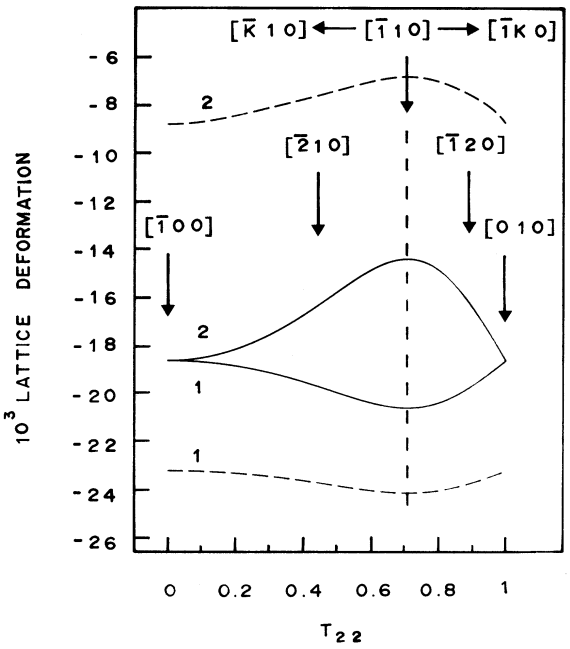

FIG. 3. Lattice deformations for different in-plane quantum-wire orientations: $[\bar{k}10]$ if $0 \le T_{22} \le 1/\sqrt{2}$ and $[\bar{1}k0]$ if $1/\sqrt{2} \le T_{22} \le 1$. The surface orientation is [001]. The solid lines refer to wires made from a single $In_{0.2}Ga_{0.8}As$ layer, while the dashed lines refer to the $In_{0.2}Ga_{0.8}As$ layers of a $GaAs/In_{0.2}Ga_{0.8}As$ QWSL, coherently fabricated on a GaAs substrate. Curves 1 show the perpendicular component of the lattice deformation, i.e., $\varepsilon_{sb} - \bar{\varepsilon}_{33}$, while curves 2 show the in-plane lattice deformation normal to the wire direction, i.e., $\varepsilon_{sb} - \bar{\varepsilon}_{11}$.

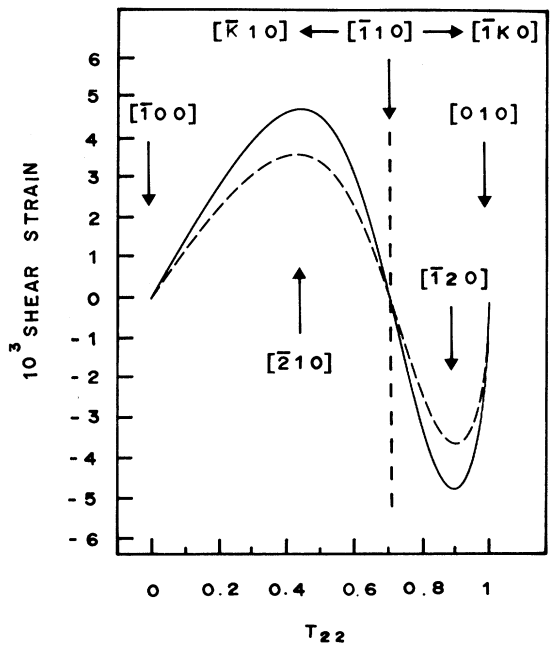

FIG. 4. Shear strain $\bar{\varepsilon}_{12}$ for different quantum-wire orientations: $[\bar{k}10]$ if $0 \le T_{22} \le 1/\sqrt{2}$ and $[\bar{1}k0]$ if $1/\sqrt{2} \le T_{22} \le 1$. The solid line refers to wires made from a single $In_{0.2}Ga_{0.8}As$ layer, while the dashed line refers to the $In_{0.2}Ga_{0.8}As$ layers of a $GaAs/In_{0.2}Ga_{0.8}As$ QWSL, coherently fabricated on a GaAs(001) substrate.

configurations for wires fabricated on a [001]-oriented substrate lead to a monoclinic lattice deformation.

B. [$\bar{1}$10]-oriented quantum wires fabricated on [$kk1$]- or [$11k$]-oriented substrates

In this subsection we will investigate the case of a fixed wire direction and a variable substrate orientation. If the chosen wire direction is $x_2' \| [\bar{1}10]$, we can put $x_3' \| [kk1]$ or $x_3' \| [11k]$. In Fig. 5 we show the lattice deformations for the following substrate orientations: $[kk1]$ with k integer if $0 \le T_{33} \le 1/\sqrt{3}$ and $[11k]$ with k integer if $1/\sqrt{3} \le T_{33} \le 1$. The solid lines are referred to a single laterally confined $In_{0.2}Ga_{0.8}As$ layer coherently fabricated on a thick GaAs substrate. Curve 2 shows the perpendicular component of the lattice deformation, i.e., $\varepsilon_{sb} - \varepsilon_{33}$, while curve 1 shows the in-plane lattice deformation orthogonal to the wire direction, i.e., $\varepsilon_{sb} - \bar{\varepsilon}_{11}$. The dashed lines are referred to the $In_{0.2}Ga_{0.8}As$ layers of a laterally confined GaAs/$In_{0.2}Ga_{0.8}As$ QWSL, coherently fabricated on a thick GaAs substrate. Here, we have assumed that the GaAs and $In_{0.2}Ga_{0.8}As$ layers have the same thickness. From this figure we can see that the in-plane and the perpendicular lattice deformations are different for any substrate orientation, except for the case of a single well fabricated on a substrate whose orientation does not belong to the $[kk1]$ or the $[11k]$ but to the more general $[hhk]$ family, with $h > 1$. Moreover, from Fig. 6 we see that, for the above considered HS, the nontrivial shear strain component goes to zero only for the high-symmetry substrate orientations [001] and [110]. Therefore, the highest possible symmetry of the deformed lattice is orthorhombic for the [001] and [110] orientations. For any other substrate orientation the lattice unit cell of the well becomes monoclinic after the deformation.

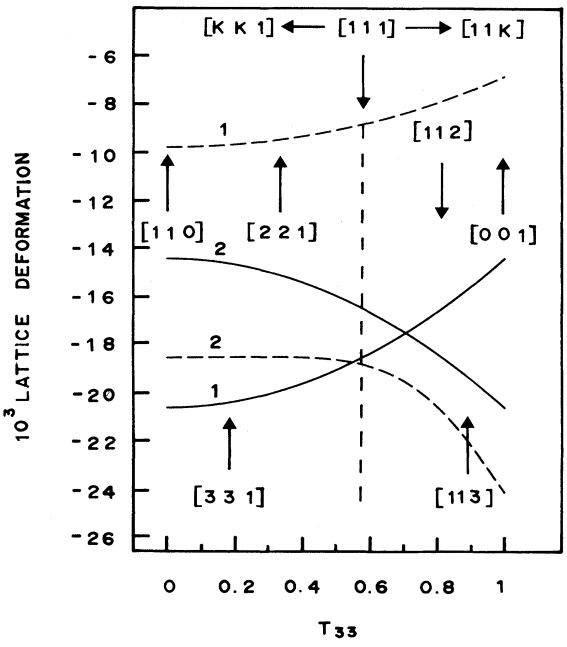

FIG. 5. Lattice deformations for two families of substrate orientations: $[kk1]$ if $0 \le T_{33} \le 1/\sqrt{3}$ and $[11k]$ if $1/\sqrt{3} \le T_{33} \le 1$. The solid lines refer to wires made from a single $In_{0.2}Ga_{0.8}As$ layer, while the dashed lines refer to the $In_{0.2}Ga_{0.8}As$ layers of a GaAs/$In_{0.2}Ga_{0.8}As$ QWSL, coherently fabricated on a GaAs substrate. Curves 1 show the in-plane lattice deformation normal to the wire direction, i.e., $\varepsilon_{sb} - \bar{\varepsilon}_{11}$, while curves 2 show the perpendicular component of the lattice deformation, i.e., $\varepsilon_{sb} - \bar{\varepsilon}_{33}$,

IV. PIEZOELECTRIC FIELDS

Zinc-blende structure semiconductors are piezoelectric materials. Elastic strain fields can induced a polarization as given by Eq. (14) of paper I of this work.[10] If we consider the case where there is no external charge, we find from the electrostatic equations that this strain-induced polarization generates an electric field orthogonal to the heterointerface.

In Fig. 7 we show the strain-induced electric fields in a quantum wire made from a single $In_{0.2}Ga_{0.8}As$ layer (curve 1) and of a GaAs/$In_{0.2}Ga_{0.8}As$ SL (curve 2), fabricated along the generic $[\bar{k}10]$ or $[\bar{1}k0]$ direction on a GaAs [001]-oriented substrate. Clearly, the presence of the GaAs barrier layers, which store a part of the strain, reduces the elastic deformation of the well lattice. Consequently, the magnitude of the strain-induced electric field is reduced with respect to the case of a single $In_{0.2}Ga_{0.8}As$ layer. It can also be seen that these electric

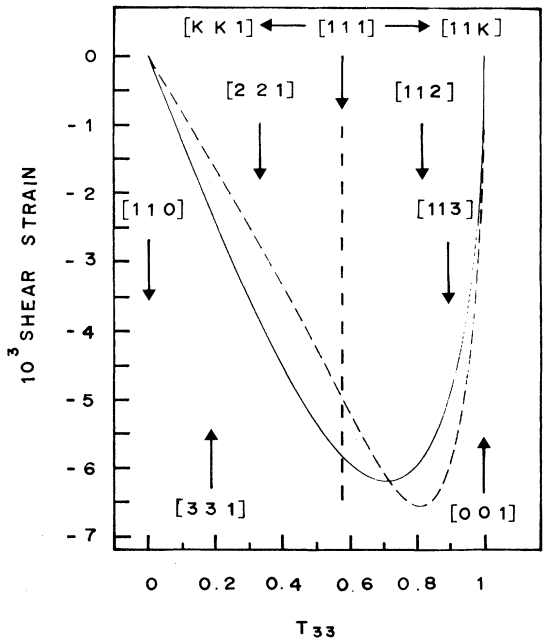

FIG. 6. Shear strain $\bar{\varepsilon}_{13}$ for two families of substrate orientations: $[kk1]$ if $0 \le T_{33} \le 1/\sqrt{3}$ and $[11k]$ if $1/\sqrt{3} \le T_{33} \le 1$. The solid line refers to wires made from a single $In_{0.2}Ga_{0.8}As$ layer, while the dashed line refers to the $In_{0.2}Ga_{0.8}As$ layers of a GaAs/$In_{0.2}Ga_{0.8}As$ QWSL, coherently fabricated on a GaAs substrate.

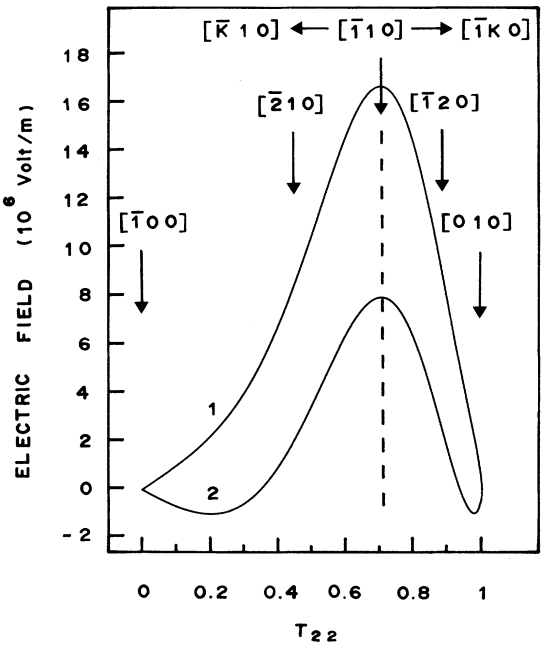

FIG. 7. Strain-induced electric fields in a quantum wire made from a single $In_{0.2}Ga_{0.8}As$ layer (curve 1) or made from a $GaAs/In_{0.2}Ga_{0.8}As$ SL (curve 2). The wires are fabricated along the generic $[\bar{k}10]$ or $[\bar{1}k0]$ directions on a GaAs [001]-oriented substrate.

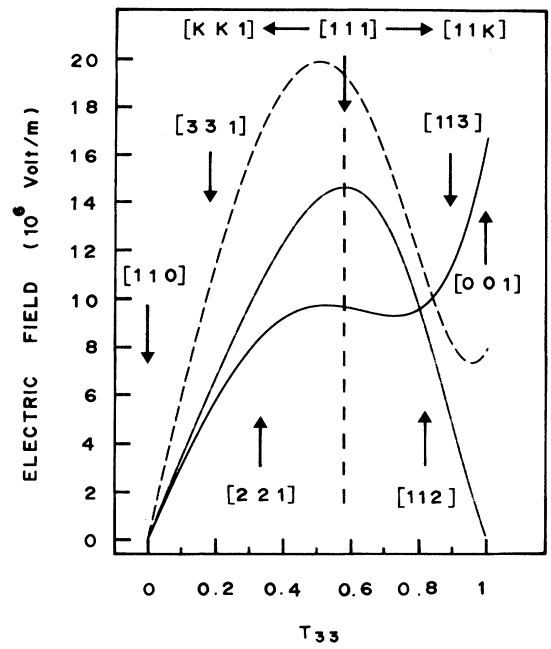

FIG. 8. Strain-induced electric fields as a function of an arbitrary interface orientation $[11k]$ or $[kk1]$ in the wells of a $GaAs/In_{0.2}Ga_{0.8}As$ $[\bar{1}10]$-oriented quantum wire deposited on a GaAs substrate (dashed line), of a free-standing $GaAs/In_{0.2}Ga_{0.8}As$ SL (dashed-dotted line) and of a $[\bar{1}10]$-oriented wire made from a single $In_{0.2}Ga_{0.8}As$ layer (solid line).

fields are zero for the wire direction with highest symmetry. This result is related to the fact that for this orientation, even after the deformation, the center of symmetry of the positive charges still coincides with that of the negative ones. In contrast, for the $[\bar{1}10]$ wire orientation the electric field reaches a pronounced maximum of the order of 10^6–10^7 V/m, for both the single-layer quantum wire and the QWSL.

In Fig. 8 we show the strain-induced electric fields in the wells of a $GaAs/In_{0.2}Ga_{0.8}As$ $[\bar{1}10]$-oriented quantum wire on a GaAs substrate (dashed line), of a $GaAs/In_{0.2}Ga_{0.8}As$ free-standing SL (dashed-dotted line), and of a $[\bar{1}10]$-oriented quantum wire on a GaAs substrate obtained by a single $In_{0.2}Ga_{0.8}As$ layer (solid line). The electric fields are presented as a function of the director cosine T_{33} of an arbitrary interface orientation $[11k]$ and $[kk1]$, where k is an integer. The most important finding is the presence of nonzero electric fields also for the [001] substrate orientation, due to the relaxation phenomena. In summary, if we are dealing with 1D structures (quantum wires) in contrast to 2D structures (SL's, multilayers), even for the surface orientation with highest symmetry, we may obtain strong piezoelectric fields different from zero, which are comparable to the spontaneous polarizations in weak ferroelectrics (i.e., Rochelle salt).[13]

V. CONCLUSIONS

In this paper, we investigated theoretically the strain and piezoelectric fields of 1D semiconductor HS's as a function of the heterointerface orientation. We show that the use of elasticity theory and the appropriate boundary conditions between wire and substrate (commensurability constraint along the wire direction and elastic lattice relaxation perpendicular to the wire direction) can lead to an orthorhombic or lower-symmetry lattice deformation also for the [001] interface orientation.

For HS's of zinc-blende structure these strain fields can generate high piezoelectric fields that for quantum wires, in contrast to 2D HS's such as SL's and multilayers, can be different from zero even for the [001] interface orientation. These static electric fields may change the microscopic band structure and have great influence on the electronic and optical properties of the constituent materials. The presence of piezoelectric fields also for the [001] interface orientation is of high interest, since this allows one to produce a one-dimensional electron (or hole) gas in a quantum-wire structure without the necessity of modulation doping and is, therefore, of great importance to the design of new devices on a nanometer scale with similar functions as conventional modulation-doped field-effect transistors.[14]

ACKNOWLEDGMENTS

The authors would like to thank Angelo Rodia for valuable assistance and Paola Leo for critical reading of the manuscript.

APPENDIX

In the following, we report on the analytical expressions of the strain-tensor components that have been obtained by minimization of the strain-energy density and by using the commensurability constraint given by Eqs. (1). The strain-tensor components $\bar{\varepsilon}_i^a$ and $\bar{\varepsilon}_i^b$ of materials a and b, respectively, expressed in the matrix notation are given by

$$
\begin{aligned}
\bar{\varepsilon}_i^a = \frac{1}{\Delta}\Bigg\{ & r\frac{d_b}{d_a}\{(\bar{S}^b_{12}\bar{S}^a_{26}-\bar{S}^a_{12}\bar{S}^b_{26})[(\bar{S}^a_{i1}\bar{S}^b_{26}-\bar{S}^a_{i6}\bar{S}^b_{12})\varepsilon_{sa}+\bar{S}^b_{26}\bar{S}^a_{i2}\varepsilon_{ba}] \\
& +\bar{S}^a_{i2}(\bar{S}^{b\,2}_{12}\bar{S}_{66}+\bar{S}^{b\,2}_{26}\bar{S}_{11}-2\bar{S}^b_{12}\bar{S}^b_{26}\bar{S}_{16})\varepsilon_{sa}+\bar{S}^b_{26}\bar{S}^a_{22}(\bar{S}^a_{i1}\bar{S}^b_{26}-\bar{S}^a_{i6}\bar{S}^b_{12})\varepsilon_{ba}\} \\
& +(\bar{S}^a_{12}\bar{S}_{66}-\bar{S}_{16}\bar{S}^a_{26})\left[\bar{S}^b_{22}(\bar{S}^a_{il}\varepsilon_{sa}+\bar{S}^a_{i2}\varepsilon_{ba})+\frac{d_b}{d_a}\bar{S}^b_{12}\bar{S}^a_{i2}\varepsilon_{sb}\right] \\
& -(\bar{S}^a_{22}\bar{S}_{66}-\bar{S}^{a\,2}_{26})\left[\bar{S}^b_{22}\varepsilon_{ba}+\frac{d_b}{d_a}\bar{S}^b_{12}\varepsilon_{sb}\right]\bar{S}^a_{il} \\
& -(\bar{S}^a_{12}\bar{S}^a_{26}-\bar{S}_{16}\bar{S}^a_{22})\left[\bar{S}^b_{22}\bar{S}^a_{i6}\varepsilon_{ba}+\frac{d_b}{d_a}(\bar{S}^a_{il}\bar{S}^b_{26}+\bar{S}^a_{i6}\bar{S}^b_{12})\varepsilon_{sb}\right] \\
& +(\bar{S}_{11}\bar{S}^a_{26}-\bar{S}_{16}\bar{S}^a_{12})\left[\frac{d_b}{d_a}\bar{S}^b_{26}\bar{S}^a_{i2}\varepsilon_{sb}+\bar{S}^b_{22}\bar{S}^a_{i6}\varepsilon_{sa}\right]+\bar{S}^a_{i6}\bar{S}^b_{26}(\bar{S}^{a\,2}_{12}-\bar{S}_{11}S^a_{22})\frac{d_b}{d_a}\varepsilon_{sb} \\
& -\bar{S}^b_{22}\bar{S}^a_{i2}(\bar{S}_{11}\bar{S}_{66}-\bar{S}^2_{16})\varepsilon_{sa}\Bigg\}, \\
\bar{\varepsilon}_i^b = \frac{r}{\Delta}\Bigg\{ & (\bar{S}^a_{22}\bar{S}_{66}-\bar{S}^{a\,2}_{26})\left[(\bar{S}^b_{i1}\bar{S}^b_{22}-\bar{S}^b_{i2}\bar{S}^b_{12})\varepsilon_{ba}+\left[\frac{d_b}{d_a}\bar{S}^b_{i1}\bar{S}^b_{12}-\frac{1}{r}\bar{S}^b_{i2}\bar{S}_{11}\right]\varepsilon_{sb}\right] \\
& +(\bar{S}_{16}\bar{S}^a_{26}-\bar{S}^a_{12}\bar{S}_{66})\left[(\bar{S}^b_{i1}\bar{S}^b_{22}-\bar{S}^b_{i2}\bar{S}^b_{12})\varepsilon_{sa}-\frac{1}{r}\bar{S}^b_{i2}\bar{S}^a_{12}\varepsilon_{sb}\right] \\
& +(\bar{S}^a_{12}\bar{S}_{16}-\bar{S}_{11}\bar{S}^a_{26})(\bar{S}^b_{22}\bar{S}^b_{i6}-\bar{S}^b_{i2}\bar{S}^b_{26})\varepsilon_{sa} \\
& +(\bar{S}^a_{12}\bar{S}^a_{26}-\bar{S}_{16}\bar{S}^a_{22})\left[(\bar{S}^b_{22}\bar{S}^b_{i6}-\bar{S}^b_{i2}\bar{S}^b_{26})\varepsilon_{ba}+\frac{d_b}{d_a}(\bar{S}^b_{i6}\bar{S}^b_{12}+\bar{S}^b_{i1}\bar{S}^b_{26})\varepsilon_{sb}-\frac{1}{r}\bar{S}^b_{i2}\bar{S}_{16}\varepsilon_{sb}\right] \\
& -\frac{d_b}{d_a}(\bar{S}^{a\,2}_{12}-\bar{S}_{11}\bar{S}^a_{22})\bar{S}^b_{i6}\bar{S}^b_{26}\varepsilon_{sb}-r\frac{d_b}{d_a}(\bar{S}^b_{i1}\bar{S}^b_{26}-\bar{S}^b_{i6}\bar{S}^b_{12})[(\bar{S}^b_{12}\bar{S}^a_{26}-\bar{S}^a_{12}\bar{S}^b_{26})\varepsilon_{sa}+\bar{S}^a_{22}\bar{S}^b_{26}\varepsilon_{ba}]\Bigg\},
\end{aligned}
\tag{A1}
$$

where $i=\{1,\ldots,6\}$ and

$$
\begin{aligned}
& r=\frac{h_a d_b}{h_b d_a}, \\
& \Delta=\left[2r\frac{d_b}{d_a}\bar{S}^b_{12}\bar{S}^b_{26}-\bar{S}_{16}\bar{S}^b_{22}\right](\bar{S}^a_{12}\bar{S}^a_{26}-\bar{S}_{16}\bar{S}^a_{22})+\left[r\frac{d_b}{d_a}\bar{S}^{b\,2}_{12}-\bar{S}^b_{22}\bar{S}_{11}\right](\bar{S}^a_{22}\bar{S}_{66}-\bar{S}^{a\,2}_{26}) \\
& \quad +r\frac{d_b}{d_a}\bar{S}^{b\,2}_{26}(\bar{S}_{11}\bar{S}^a_{22}-\bar{S}^{a\,2}_{12})-\bar{S}^b_{22}\bar{S}^a_{12}(\bar{S}_{16}\bar{S}^a_{26}-\bar{S}^a_{12}\bar{S}_{66}), \\
& \varepsilon_{ba}=\frac{d_b-d_a}{d_a}, \\
& \varepsilon_{s\alpha}=\frac{d_s-d_\alpha}{d_\alpha}, \\
& \bar{S}_{ij}\equiv\bar{S}^a_{ij}+r\frac{d_b}{d_a}\bar{S}^b_{ij}.
\end{aligned}
\tag{A2}
$$

Here, $\bar{S}_{ij}^{\alpha}$ are the compliance tensor elements of the layer $\alpha=\{a,b\}$ calculated with respect to the interface reference system, and h_a and h_b are the thicknesses of layers a and b, respectively. In the Appendix of paper I of this work (Ref. 10) are reported the explicit expressions of these compliance components as a function of the stiffness tensor elements and the transformation matrix elements T_{ik}.

---

[1]C. P. Duo, S. K. Vong, R. M. Cohen, and G. B. Stringfellow, J. Appl. Phys. **57**, 5428 (1985).
[2]J. M. Hinckley and J. Singh, Phys. Rev. B **42**, 3546 (1990); Appl. Phys. Lett. **60**, 2694 (1991).
[3]C. Mailhiot and D. L. Smith, Phys. Rev. B **35**, 1242 (1987); Rev. Mod. Phys. **62**, 173 (1990).
[4]L. De Caro and L. Tapfer, Phys. Rev. B **48**, 2298 (1993).
[5]L. Tapfer, G. C. La Rocca, H. Lage, O. Brandt, D. Heitmann and K. Ploog, Appl. Surf. Sci. **60/61**, 517 (1992).
[6]L. Tapfer, G. C. LaRocca, H. Lage, R. Cingolani, P. Grambow, A. Fischer, D. Heitmann, and K. Ploog, Surf. Sci. **267**, 227 (1992).
[7]M. M. J. Treacy and M. Gibson, J. Vac. Sci. Technol. B **4**, 1458 (1986).
[8]L. De Caro and L. Tapfer, Phys. Rev. B **49**, 11 127 (1994).
[9]L. De Caro and L. Tapfer (unpublished).
[10]L. De Caro and L. Tapfer, preceding paper, Phys. Rev. B **51**, 4374 (1995).
[11]J. F. Nye, *Physical Properties of Crystals* (Oxford University Press, Oxford, 1964), pp. 93–109 and 131–149.
[12]*Semiconductors: Physics of Group IV Elements and III-V Compounds,* edited by O. Madelung, Landolt-Börnstein, New Series, Group III, Vol. 17, Pt. a (Springer, Berlin, 1991).
[13]*Ferroelectrics and Related Substances,* edited by K. H. Hellwege, Landolt-Bornstein, New Series, Group III, Vol. 16, Pt. a (Springer-Verlag, Berlin, 1981).
[14]E. S. Snow, B. V. Shanabrook, and D. Gammon, Appl. Phys. Lett. **56**, 758 (1990).